ELSEVIER

Inorganica Chimica Acta 226 (1994) 231–235

Inorganica Chimica Acta

Free radical-mediated electron transfer in organometallic complexes: homolysis and alkyl group crossover reactions for alkyliron(II) porphyrins

Byungho Song, Harold M. Goff *

Department of Chemistry, University of Iowa, Iowa City, IA 52242, USA

Received 1 June 1994

Abstract

Alkyliron(III) porphyrin iron–carbon bond homolysis at ambient temperature yields a putative steady-state concentration of alkyl radicals. Homolytic decomposition by radical coupling and other reactions becomes auto-limiting due to competitive capture of subsequently formed alkyl radicals by the iron(II) porphyrin product. This reaction sequence is supported by radical-transfer crossover reactions in which the alkyl ligand of an alkyliron(III) porphyrin is transferred to another iron(II) porphyrin of different structure.

Keywords: Free radical transfer; Bond homolysis; Iron complexes; Alkyl complexes; Porphyrin complexes

1. Introduction

Five-coordinate alkyl- and aryliron(III) porphyrin complexes are readily generated under anaerobic conditions by stoichiometric addition of Grignard or lithium reagents to the chloroiron(III) porphyrin [1]. The iron(III)–carbon bond energies are seemingly lower than those of the cobalt(III) analogues that serve as models for vitamin B_{12} free-radical chemistry. Paramagnetic organometallic iron(III) porphyrin complexes are quite reactive and exhibit a variety of unusual and unprecedented reactions exemplified by the following: (i) reversible migration of the alkyl/aryl ligand from the metal center to a porphyrin pyrrole nitrogen [2]; (ii) hydrometallation of alkynes to give σ-vinyliron(III) porphyrins [3]; (iii) 'insertion' of dioxygen into the Fe–C bond of alkyl/aryliron(III) porphyrins to give a transient organic peroxide complex [4]; (iv) 'insertion' of CO [5,6], CO_2 [5] and SO_2 [7] into the Fe–C bond of alkyliron(III) porphyrins; (v) a novel alkyl group free radical 'interchange' with alkyl halides [8]; (vi) formation of a tributyltin–iron(III) porphyrin complex from tributyltin hydride and an alkyliron(III) porphyrin [9]; (vii) 'insertion' of carbon disulfide into the alkyl–iron(III) bond to give an unusual dithioformylester complex [10].

Mechanistic investigations of reactions (iv)–(vii) give a consistent picture of facile thermal homolysis of the Fe–C bond as the initial step of the diverse reaction types [5,6,8].

$$\text{(P)Fe(III)–R} \rightleftharpoons \text{(P)Fe(II)} + {}^{\bullet}\text{R} \qquad (1)$$

The reverse reaction rate is expected to approach diffusion-control on the basis of pulsed radiolysis measurements [11]. Thus, solutions of alkyliron(III) porphyrins provide an ambient temperature steady-state source of free radicals (aryl complexes are relatively more stable [1]). The thermal homolytic process for alkyliron(III) porphyrins is analogous to the 'persistent radical effect' described for an alkylcobalt(III) macrocycle [12,13].

Radical loss by combination, disproportionation, etc., accounts for the instability of alkyliron(III) porphyrins.

$$(n)^{\bullet}\text{R} \longrightarrow \text{alkanes, alkenes} \qquad (2)$$

The iron(II) product appears over a period of hours to days and the irreversible decomposition rate is dependent on the porphyrin ring basicity. In non-coordinating solvents such as benzene, toluene and dichloromethane the iron(II) porphyrin remains as the square-planar species [14]. This iron(II) product could presumably react with the alkyl radical produced by thermal homolysis and effectively favor the reverse process in reaction (1). Hence, the net decomposition

* Corresponding author.

SSDI 0020-1693(94)04090-I

process is expected to be self-inhibitory due to favorable radical capture by the iron(II) product. Results described here do indeed reveal an unusual limiting decomposition rate.

The hypothetical capture of alkyl radicals by iron(II) porphyrins has also been evaluated further by experiments that show a 'crossover' of alkyl group between porphyrins of differing structural type. This transfer of an alkyl ligand between iron porphyrins confirms that the alkyl radical is not confined to a radical 'cage' of the parent complex.

2. Experimental

The previously described chloroiron(III) tetraarylporphyrin compounds were prepared by aldehyde/pyrrole condensation [15] or purchased from Aldrich Chemical Co. The pyrrole-deuterated derivatives were prepared by pyrrole deuterium exchange prior to macrocycle condensation [16]. Optical and NMR spectroscopies were used to verify the integrity of the complexes.

Ethyl- and butyliron(III) porphyrin complexes were generated in benzene or toluene solution under anaerobic (glove box) conditions. The in situ metathesis reactions were conducted by addition of a measured volume of ethylmagnesium bromide solution (1.0 M in THF, Aldrich) or butyllithium solution (2.0 M in pentane, Aldrich) to the previously weighed chloroiron(III) porphyrin dissolved in the aromatic solvent in a 5 mm NMR tube. Initial stability experiments were also conducted with ethyliron(III) porphyrins prepared by addition of 1.0 molar equivalent of sodium triethylborohydride (1.0 M in THF, Aldrich). Ethyl group transfer rather than hydride transfer is evident. The stability results showed no difference for ethyliron(III) porphyrin generated from the Grignard reagent or triethylborohydride. In situ generation of the unstable complexes was utilized, as isolation of crystalline product [1] and redissolution gave larger quantities of homolyzed and μ-oxo iron(III) dimeric byproducts.

Following generation of the alkyliron(III) complex, the 5 mm NMR tube was sealed with either a rubber septum, or for the extended decomposition studies, J. Young NMR tubes (Wilmad Co.) were utilized. Samples used for decomposition studies were stored in the glove box and protected from light during the course of the reaction.

Iron(II) porphyrins were generated in toluene solution by reduction of the chloroiron(III) analogue through vigorous stirring with mercury-activated zinc powder [17]. Filtered solutions of the iron(II) porphyrin were utilized directly for the crossover experiments.

3. Results and discussion

3.1. Decomposition reactions

The influence of porphyrin ring basicity on the decomposition of alkyliron(III) tetraarylporphyrins was investigated qualitatively by proton NMR integration of the porphyrin pyrrole and coordinated ethyl-CH_3 signal intensities. These signals for the paramagnetic, low-spin ethyliron(III) porphyrin compounds (structures shown in Fig. 1) are in the far upfield region [8]. The following respective pyrrole and CH_3 chemical shift values were measured for 4 mM toluene solutions (25 °C, TMS reference): (p-OCH_3TPP)Fe(III)CH_2CH_3, −17.5 and −115 ppm; (TPP)Fe(III)CH_2CH_3, −17.6 and −117 ppm; (F_8-TPP)Fe(III)CH_2CH_3, −19.5 and −124 ppm; (F_{20}-TPP)Fe(III)CH_2CH_3, −20.1 and −126 ppm. Signal intensities decreased to 50% of the original value over respective periods of 4 days, 3.5 days, 2 days and 45 min. Signals for the corresponding iron(II) porphyrins partially complexed with THF (from the triethylborohydride or Grignard reagent used to generate the ethyl complex) increased in intensity as the ethyliron(III) complex decomposed.

The qualitative stability order is related to porphyrin ring basicity. More basic porphyrins favor the iron(III) oxidation state, whereas the more electron-deficient halogenated porphyrins serve to stabilize the iron(II) oxidation state. The equilibrium expressed by Eq. (1) lies further to the right for the electron deficient porphyrins, the steady-state free radical concentration should be higher, and irreversible radical loss by an Eq. (2) process is associated with faster 'decomposition'. Organometallic iron(III) porphyrin complexes prone to homolytic decomposition can obviously be stabilized by choice of more basic porphyrin substituents.

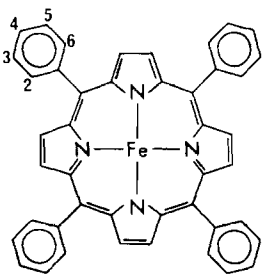

Fig. 1. Iron porphyrin structures.

Abbreviation	Phenyl ring position substituents				
	2	3	4	5	6
(TPP)Fe	H	H	H	H	H
(p-OCH_3TPP)Fe	H	H	-OCH_3	H	H
(F_8-TPP)Fe	F	H	H	H	F
(F_{20}-TPP)Fe	F	F	F	F	F

Decomposition of (TPP)Fe(III)CH_2CH_3 in toluene solution was investigated further as a function of iron porphyrin concentration. Concentrations of 8.6, 1.8 and 0.62 mM (TPP)Fe(III)CH_2CH_3 were employed (concentrations were determined by initial weight of (TPP)Fe(III)Cl and relative integration of signals for the (TPP)Fe(III)CH_2CH_3 product). Proton NMR spectra were recorded periodically over a period of more than one month. In order to maintain rigorous anaerobic conditions the samples were stored in the glove box at 23 ± 2 °C between NMR spectral acquisitions. The absence of a 13.5 ppm signal for the pyrrole proton of (TPP)Fe(III)–O–Fe(III)(TPP), a characteristic product from air exposure of the (TPP)Fe(II) homolytic decomposition species, gave a positive indication of the anaerobic integrity. The −17.6 ppm pyrrole proton signal of (TPP)Fe(III)CH_2CH_3 was integrated for comparison with well resolved *meta/para*- and *ortho*-phenyl signals at 12.7 and 20.5 ppm for the (TPP)Fe(II) product. In order to simplify comparisons for the differing initial concentrations, the ratio of remaining (TPP)Fe(III)-CH_2CH_3 to total iron porphyrin was calculated from integrated intensities at various times. Data are presented in Fig. 2. with ratios converted to percentages. It is evident that decomposition levels off and that the fraction of (TPP)Fe(III)CH_2CH_3 remaining is a function of the initial concentration. This unusual observation is fully consistent with processes described by Eqs. (1) and (2). The (TPP)Fe(II) generated by decomposition of the initial portion of the alkyliron(III) porphyrin complex serves as an efficient radical 'trap' for subsequent homolysis. The trap reaction corresponds to the reverse step in Eq. (1). Hence, the decomposition is greatly attenuated after appearance of a sufficient concentration of the iron(II) derivative.

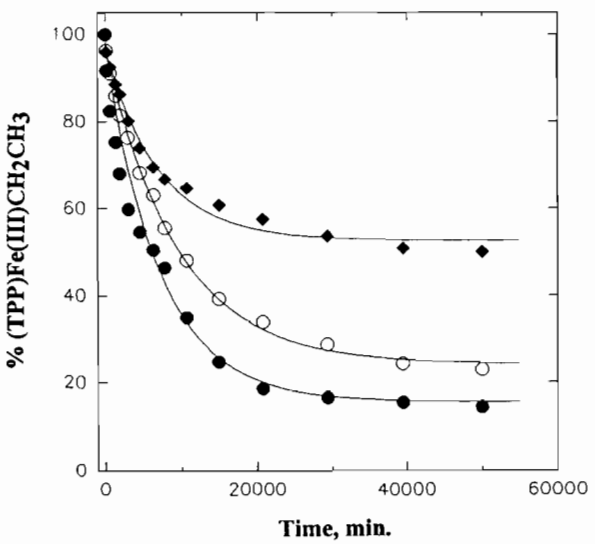

Fig. 2. Time dependence of (TPP)Fe(III)CH_2CH_3 decomposition. Toluene solution, 23 ± 2 °C. Initial concentration of (TPP)FeCH_2CH_3: ◆, 8.6; ○, 1.8; ●, 0.62 mM. Curves reflect the best fit for first-order.

The kinetic profile for decomposition is expected to be quite complex. However, reasonable fits for a first-order process are reflected in the curves in Fig. 2. Apparent first-order rate constants for the highest to lowest concentrations are 1.4×10^{-4}, 1.1×10^{-4} and 1.4×10^{-4} min^{-1}, respectively. It should be emphasized that these observed rate constants are the product of several terms, and do not give a direct measure of the rate of reaction (2). The important point is that the observed decomposition rate appears to be independent of the initial (TPP)Fe(III)CH_2CH_3 concentration.

Other mechanisms were given consideration in an attempt to explain the plateau in alkyliron(III) porphyrin decomposition. The presence of a solvent contaminant (reducing agent) at a sub-stoichiometric concentration with respect to the iron porphyrin would cause partial 'decomposition'. However, this mechanism is incompatible with the differing absolute amounts of (TPP)Fe(III)CH_2CH_3 decomposed as the initial concentration is varied. A specific role for toluene as a solvent was also considered. Benzyl radical formation is plausible. However, the unstable benzyliron(III) porphyrin complex was never detected, and moreover, use of benzene as a solvent gave the same decomposition profile as that for toluene.

3.2. Crossover reactions

The facile homolytic mechanism described by Eq. (1) suggests that an alkyl radical escaping the radical cage could be 'trapped' by a second, structurally different iron(II) porphyrin. The iron porphyrin trap would be converted to the alkyliron(III) form and exhibit a distinctive upfield pyrrole proton (or deuteron) NMR signal. Such a reaction sequence is indeed evident in the progression of the proton NMR spectra shown in Fig. 3. Spectra were acquired over a period of hours after combination of approximately one equivalent of (TPP)Fe(III)$(CH_2)_3CH_3$ (and one equivalent of (TPP)Fe(III)Cl, see discussion below) with two equivalents of (F_{20}-TPP)Fe(II) in toluene solutions. Compounds with widely differing electronic properties were chosen in order to preclude any direct reduction of the alkyliron(III) porphyrin by the iron(II) porphyrin. During the course of the reaction the original pyrrole proton signal for (TPP)Fe(III)$(CH_2)_3CH_3$ at −18.3 ppm (peak a) is partially replaced by the pyrrole proton signal for (F_{20}-TPP)Fe(III)$(CH_2)_3CH_3$ at −20.5 ppm (peak b). The following equilibrium is established over a period of an hour.

$$(TPP)Fe(III)(CH_2)_3CH_3 + (F_{20}\text{-}TPP)Fe(II) \rightleftharpoons (TPP)Fe(II) + (F_{20}\text{-}TPP)Fe(III)(CH_2)_3CH_3 \quad (3)$$

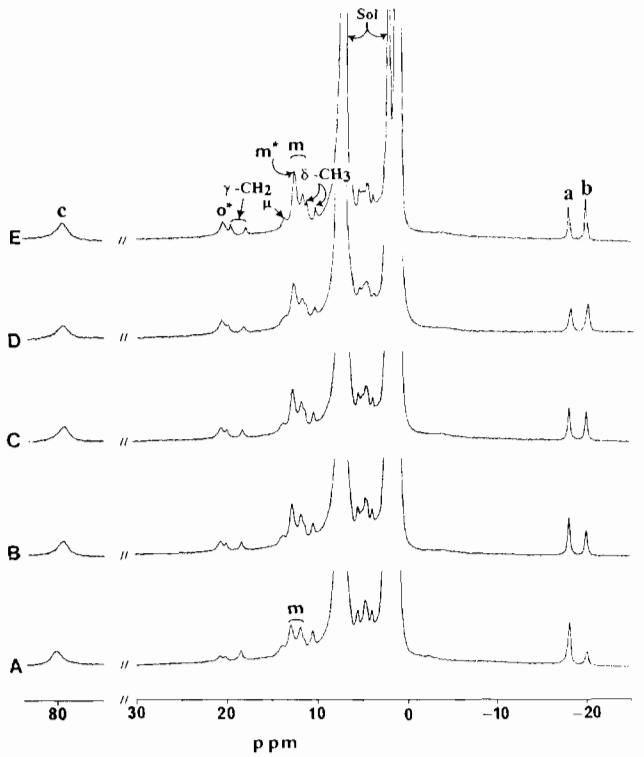

Fig. 3. Proton NMR spectra for the alkyl ligand crossover reaction. Toluene-d_8 solution, 25 °C, TMS reference, spectra recorded at 360 MHz. Initial concentrations (after mixing): (TPP)Fe(III)$(CH_2)_3CH_3$, 1.0 mM; (TPP)Fe(III)Cl, 1.0 mM; (F_{20}-TPP)Fe(II), 2.0 mM. Signal assignments are discussed in the text. The μ peak is due to the pyrrole signal of a small contaminant of (TPP)Fe(III)–O–Fe(III)-(TPP). Spectra were recorded at the following times after mixing alkyliron(III) and iron(II) solutions in the glove box: A, 10; B, 20; C, 40; D, 70; E, 180 min.

The upfield pyrrole proton signals are of comparable intensity at equilibrium. This indicates, contrary to expectations, that the two iron porphyrin compounds show much the same Fe–C bond energy. Calculation of the apparent equilibrium constant is unwarranted, however, as fractional loss of alkyl radical by Eq. (2) processes and inability to integrate iron(II) porphyrin pyrrole signals in the 5 ppm region leaves the total iron(II) and iron(III) porphyrin concentrations undefined at equilibrium.

Aside from the strong, overlapping solvent and pentane (from the butyllithium reagent) signals in the usual diamagnetic region, assignments of other signals in Fig. 3 should be noted. The broad signal at 80 ppm (peak c) and the doublet at 11.6/12.7 ppm (peaks m) are due to the pyrrole and *meta*-phenyl protons of unreacted (TPP)Fe(III)Cl, respectively [14]. In this instance a limiting amount of butyllithium (0.5 equiv.) was utilized in order to insure that no free butyllithium remained after generation of (TPP)Fe(III)$(CH_2)_3CH_3$. Free butyllithium would have precluded identification of a crossover reaction. Hence, the reaction mixture initially contained a 1:1 ratio of (TPP)Fe(III)Cl and (TPP)Fe(III)$(CH_2)_3CH_3$ (2 mM each) to which was added an equal volume of 4 mM (F_{20}-TPP)Fe(II). It should be noted that intensities of pyrrole and phenyl proton signals of (TPP)Fe(III)Cl did not change during the reaction. Furthermore, the same alkyl radical crossover phenomenon was observed for separate experiments (not shown) in which none of the parent (TPP)Fe(III)Cl was present.

Downfield phenyl proton signals for (TPP)Fe(II) appeared during the course of the reaction. These are assigned to the *ortho*-phenyl proton at 20.5 ppm (peak o*), and the *meta-/para*-phenyl protons at 12.7 ppm (peak m*) [14]. The γ-CH_2 protons of the coordinated butyl ligand exhibit a resolved signal at 18.3 ppm for the (TPP)Fe(III)$(CH_2)_3CH_3$ complex, and as the reaction proceeds, the corresponding ligand signal for the (F_{20}-TPP)Fe(III)$(CH_2)_3CH_3$ complex is seen at 19.9 ppm. Likewise, coordinated butyl δ-CH_3 signals are seen for the respective complexes at 10.3 and 11.2 ppm. It should be noted that the intensity ratios for these two sets of ligand signals match those for the corresponding upfield set of pyrrole proton signals. Several of the proton resonances for the various complexes are obscured by strong solvent signals in the 0–9 ppm region. These include the *ortho*- and *para*-phenyl signals for (TPP)Fe(III)Cl, the phenyl signals for (TPP)Fe(III)$(CH_2)_3CH_3$, and the pyrrole signals for (TPP)Fe(II) and (F_{20}-TPP)Fe(II). The coordinated butyl β-CH_2 signals (not shown) appear at −64.9 and −63.6 ppm for the respective (TPP)Fe(III)$(CH_2)_3CH_3$ and (F_{20}-TPP)Fe(III)$(CH_2)_3CH_3$ complexes. No attempts were made to detect the coordinated butyl α-CH_2 signals which presumably are in the 600 ppm region [8].

The equilibrium described by Eq. (3) can be reached by combination of species shown on the right side of the equation. Fig. 4 shows the series of deuterium NMR spectra used to monitor the reaction. In this instance the deuterium label has been placed only at the pyrrole positions of the reactant (d_8-TPP)Fe(II). No signals are seen for the (F_{20}-TPP)Fe species, phenyl groups of the (d_8-TPP)Fe complexes, or for the butyl ligands. Deuterium NMR spectroscopy does permit observation of a pyrrole signal at 5.8 ppm for the pyrrole deuteron of (d_8-TPP)Fe(II). This signal shrinks over the course of the reaction as the pyrrole signal for (d_8-TPP)Fe(III)$(CH_2)_3CH_3$ at −18.3 ppm grows. The ratio of pyrrole signal intensities at equilibrium is 3:2 for iron(III):iron(II) derivatives. The reactants were combined in equimolar quantities, and hence the equilibrium favors (TPP)Fe(III)$(CH_2)_3CH_3$ slightly over (F_{20}-TPP)Fe(III)$(CH_2)_3CH_3$. Analogous results were obtained by combination of (TPP)Fe species with (F_8-TPP)Fe derivatives.

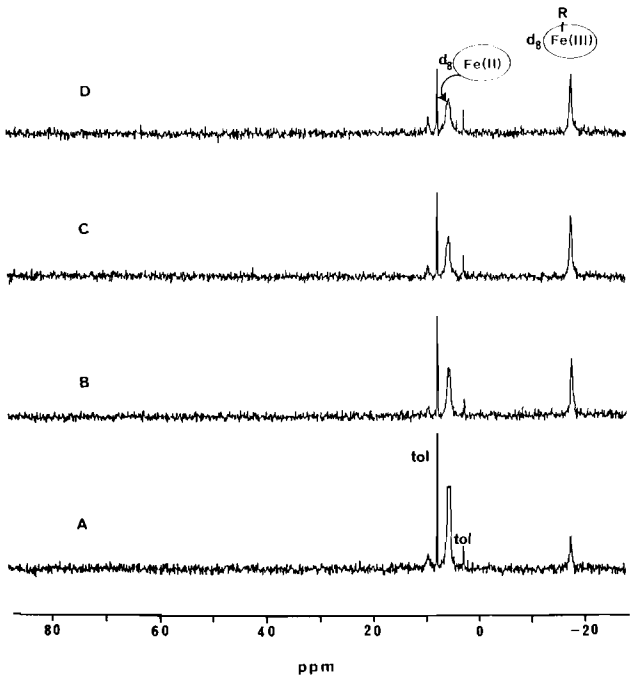

Fig. 4. Deuterium NMR spectra for the reaction of (pyrrole-d_8-TPP)Fe(II) with $(F_{20}$-TPP)Fe(III)$(CH_2)_3CH_3$. Initial concentrations of each reactant 2 mM after mixing toluene solutions. Recorded at 25 °C, 55 MHz operating frequency, TMS reference. Times after mixing reactants: A, 20; B, 70; C, 170; D, 315 min.

4. Conclusions

Results provided here support previous descriptions of alkyliron(III) porphyrin reactivity that in selected cases is derived from free radical production by a very facile, reversible Fe–C bond homolysis. The absolute homolysis rate has not been determined, but the cross-over experiments suggest diffusion from the radical cage on a time frame of minutes to tens of minutes. This is also the same time scale for CO and CS_2 'insertion' reactions, and for tributyltin hydride and iodoalkane Fe–C bond metathesis reactions. Alkyliron(III) porphyrins provide an ambient temperature steady-state source of free radicals that may be of utility for free radical initiation and rearrangement reactions.

Acknowledgement

Acknowledgement is made to the donors of the Petroleum Research Fund, administered by the American Chemical Society, for support of this research.

References

[1] P. Cocolios, G. Lagrange and R. Guilard, *J. Organomet. Chem., 253* (1983) 65.
[2] (a) H.M. Goff and M.A. Phillippi, *Inorg. Nucl. Chem. Lett., 17* (1981) 239; (b) L. Latos-Grazynski, R.-J. Cheng, G.N. La Mar and A.L. Balch, *J. Am. Chem. Soc., 103* (1981) 4270; (c) B. Chevrier, R. Weiss, M. Lange, J.-C. Chottard and D. Mansuy, *J. Am. Chem. Soc., 103* (1981) 2899; (d) P.R. Ortiz de Montellano, K.L. Kunze and O. Augusto, *J. Am. Chem. Soc., 104* (1982) 3545; (e) D. Mansuy, J.-P. Battioni, D. Dupre and E. Sartori, *J. Am. Chem. Soc., 104* (1982) 6159; (f) D. Lacon, P. Cocolios, R. Guilard and K.M. Kadish, *J. Am. Chem. Soc., 106* (1984) 4472.
[3] J. Setsune, Y. Ishimaru and A. Sera, *J. Chem. Soc., Chem. Commun.,* (1992) 328.
[4] (a) R.D. Arasasingham, A.L. Balch and L. Latos-Grazynski, *J. Am. Chem. Soc., 109* (1987) 5846; (b) R.D. Arasasingham, A.L. Balch, C.R. Cornman and L. Latos-Grazynski, *J. Am. Chem. Soc., 111* (1989) 4357; (c) A.L. Balch, R.L. Hart, L. Latos-Grazynski and T.G. Traylor, *J. Am. Chem. Soc., 112* (1990) 7382; (d) R.D. Arasasingham, A.L. Balch, R.L. Hart and L. Latos-Grazynski, *J. Am. Chem. Soc., 112* (1990) 7566; (e) A.L. Balch, M.M. Olmstead, N. Safari and T.N. St. Claire, *Inorg. Chem., 33* (1994) 2815.
[5] I.M. Arafa, K. Shin and H.M. Goff, *J. Am. Chem. Soc., 110* (1988) 5228.
[6] C. Gueutin, D. Lexa, M. Momenteau and J.-M. Saveant, *J. Am. Chem. Soc., 112* (1990) 1874.
[7] P. Cocolios, E. Laviron and R. Guilard, *J. Organomet. Chem., 228* (1982) C39.
[8] Z. Li and H.M. Goff, *Inorg. Chem., 31* (1992) 1547.
[9] B. Song and H.M. Goff, *Inorg. Chem.,* in press.
[10] B. Song and H.M. Goff, unpublished results.
[11] D. Brault, C. Bizet, P. Morliere, M. Rougee, E.J. Land, R. Santus and A.J. Swallow, *J. Am. Chem. Soc., 102* (1980) 1015.
[12] B.E. Daikh and R.G. Finke, *J. Am. Chem. Soc., 114* (1992) 2938.
[13] H. Fischer, *J. Am. Chem. Soc., 108* (1986) 3925.
[14] F.A. Walker and U. Simonis, in L.J. Berliner and J. Reuben (eds.), *Biological Magnetic Resonance,* Vol. 12, Plenum, New York, 1993, Ch. 4, p. 133.
[15] A.D. Adler, F.R. Longo, J.D. Finarelli, J. Goldmacher, J. Assour and L. Korsakoff, *J. Org. Chem., 32* (1967) 476.
[16] A. Shirazi and H.M. Goff, *J. Am. Chem. Soc., 104* (1982) 6318.
[17] J.T. Landrum, K. Hatano, W.R. Scheidt and C.A. Reed, *J. Am. Chem. Soc., 102* (1980) 6729.